

Fully Automated Inside Body WDT Transmitter Design and Optimization Through Artificial Intelligence-Based GANs and DNNs

Original

Fully Automated Inside Body WDT Transmitter Design and Optimization Through Artificial Intelligence-Based GANs and DNNs / Kouhalvandi, Lida; Matekovits, Ladislau. - In: IEEE ANTENNAS AND WIRELESS PROPAGATION LETTERS. - ISSN 1536-1225. - ELETTRONICO. - 24:4(2025), pp. 963-967. [10.1109/lawp.2024.3523379]

Availability:

This version is available at: 11583/2998982 since: 2025-04-09T16:40:14Z

Publisher:

IEEE

Published

DOI:10.1109/lawp.2024.3523379

Terms of use:

This article is made available under terms and conditions as specified in the corresponding bibliographic description in the repository


Publisher copyright

IEEE postprint/Author's Accepted Manuscript

©2025 IEEE. Personal use of this material is permitted. Permission from IEEE must be obtained for all other uses, in any current or future media, including reprinting/republishing this material for advertising or promotional purposes, creating new collecting works, for resale or lists, or reuse of any copyrighted component of this work in other works.

(Article begins on next page)

Fully Automated Inside Body WDT Transmitter Design and Optimization through Artificial Intelligence-based GANs and DNNs

Lida Kouhalvandi , Senior Member, IEEE, and Ladislau Matekovits , Senior Member, IEEE

Abstract—Biomedical inside body wireless data transfer (WDT) interface includes the design of power amplifiers (PAs) with implantable antenna leading to operate concurrently. Hence, active and passive devices are utilized simultaneously for which the accurate starting points for designing these high dimensional devices is critical. From another point of view, accelerating the design and optimization process is another substantial issue that must be considered effectively. In this study, we propose a methodology that includes two optimization phases that are applied sequentially. In the first phase, the PA is designed and optimized by employing a generative adversarial network (GAN) for predicting the load-pull contours on the Smith chart and using a long short-term memory (LSTM)-based deep neural network (DNN) for achieving the optimal design parameters of the biomedical amplifier. In this step, the GAN leads to predicting the optimal impedances needed to construct the initial structure of PA through a simplified real frequency technique. In the second optimization phase, the initial structure of the biomedical antenna is constructed automatically by developing a visual basic (VBA) environment, then like the PA, the design parameters of the antenna are optimized through the LSTM-based DNN. Finally, another GAN is generated for predicting the radiation patterns of the antenna. In both phases, a multi-objective ant lion optimizer (MOALO) is employed in the output layer of DNNs for optimizing various outcome specifications. The proposed method is performed fully automatically: active and passive devices are designed and optimized with the help of GANs and DNNs in which the drawback of heavy reliance of the system performance on the designer's experience is solved in a fast way. The proposed method is validated by designing and optimizing a biomedical PA with an antenna working at the center frequency of 2.45 GHz which shows reliable outcomes.

Index Terms—Biomedical, deep neural network (DNN), inside body wireless data transfer (WDT), generative adversarial network (GAN), multi-objective optimization.

I. INTRODUCTION

Continuous monitoring of vital signs can greatly benefit biomedical implants for which semiconductor technology is helping to improve the overall performance [1], [2]. Hence, implantable medical devices are developing exponentially leading to diagnosing, treating, and monitoring diseases and patients

[3]. The wireless data transfer (WDT) interface for biomedical applications includes both active devices (i.e., power amplifiers (PAs)) and also passive devices (i.e., antennas). For the active devices, the executed transistor's performance information is obtained through nonlinear and/or load-pull measurements [4]. Practical assessments for many impedance points is a challenging task; hence, engineers make use of software-based nonlinear device models [5]. For passive devices, electromagnetic (EM) modeling is typically based on the designer's experience which requires enormous manual work [6].

Recently, the machine learning (ML) technique has demonstrated [7]–[10] its effectiveness in biomedical wireless systems [11], [12] and it has proven its worth in substantially reducing the design workload with acceptable accuracy performance [13], [14] for high-dimensional radio frequency designs. Typically, the appropriate outcomes are obtained by separating the system into diverse designs [15], similar to domain decomposition, here thought to be at the component level. By studying the very recent publications from [1] to [6] and [16]–[19], it is observed that the concept proposed here is missing. In this study we employ various neural networks for designing and optimizing the biomedical amplifier and antenna, sequentially in an automated environment (generated between an electronic design automation (EDA) tool and numerical analyzer). In the design of a biomedical amplifier, firstly the generative adversarial network (GAN) is employed for predicting an entire set of Smith chart load-pull contours. Afterward, the extrapolated optimal gate and drain impedances are inserted into the simplified real frequency technique (SRFT) for obtaining the initial structure of PA [20]. Later, the long short-term memory (LSTM)-based deep neural network (DNN) is trained and constructed in which the multi-objective ant lion optimizer (MOALO) [21]–[23] is executed. The constructed DNN is targeted to optimize the PA in terms of S-parameter (S_{11}), drain efficiency (η_D), output power (P_{out}), power gain (G_p), and amplitude-to-phase modulation (AM/PM) specifications where the input specification of LSTM-based DNN are width (W) and length (L) of transmission lines (TLs) the antenna is built of. In the second phase, the initial structure of the biomedical antenna is constructed automatically by the combination of visual basic (VBA) environment in the CST software and also numerical analyzer as MATLAB. Afterward, the biomedical antenna is optimized by training the LSTM-based DNN leading to optimize the biomedical antenna in terms of S_{11} where like the PA the input specifications are 'W' and 'L' of the

Manuscript submitted****

(Corresponding author: ladislau.matekovits@polito.it).

L. Kouhalvandi is with the Department of Electrical and Electronics Engineering, Dogus University, Istanbul 34775, Turkiye.

L. Matekovits is with the Department of Electronics and Telecommunications, Politecnico di Torino, 10129 Torino, Italy also with the Istituto di Elettronica e di Ingegneria dell'Informazione e delle Telecomunicazioni, National Research Council of Italy, 10129 Turin, Italy and with the Department of Measurements and Optical Electronics, Politehnica University Timișoara, 300006 Timișoara, Romania.

biomedical antenna with the feeding position (x,y) , by the help of MOALO algorithm implementation. The second GAN network is trained for the biomedical antenna leading to the prediction of the E-plane and H-plane radiation pattern (RP) specifications for the whole bandwidth for diverse frequencies. All the optimization processes (i.e., including biomedical PA and antenna designs) are executed in a fully automated environment without any manual interruptions leading to: i) the construction of the initial configurations of active and passive devices with ii) optimizing the output specifications through diverse neural networks such as GANs and LSTM-based DNNs. This approach results in reducing the computation time sufficiently.

II. MODELING METHODOLOGY

The inside body WDT transmitter includes PA as an active device and antenna as a passive device, sequentially. Hence, this section is devoted to presenting the proposed methodology for designing and optimizing these high-dimensional circuits in terms of included design parameters. Here, two different network types GAN and LSTM-based DNN are employed. In both the design and optimization of PA with antenna, the GANs (as the image completion process [24]) are used for predicting data that is based on the counters. The LSTM-based DNNs [25] at both sides are also employed for predicting the various design parameters including 'W' and 'L' leading to optimizing targeted output specifications.

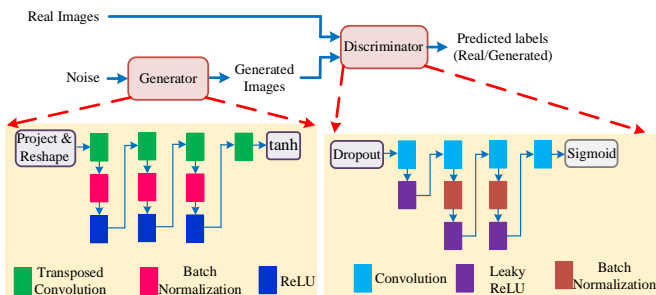


Figure 1: General structure of proposed GAN used in both modeling of biomedical PA and antenna designs.

For designing a biomedical PA, firstly an automated environment between EDA tools such as ADS and numerical analyzer as MATLAB is created (Step-1). Afterward, the GAN is employed for predicting full load-pull contours by making use of a partial dataset. Hence from the known impedances, the overall image is completed via a gradient search [26], [27]. Figure 1 shows the general structure of GAN which includes the generator network and discriminator network (Step-2). In this step, the generator network is constructed for generating valid load-pull contours and load-pull images, where the discriminator learns about realizing valid load-pull contours. After achieving the optimal drain and gate impedances through GAN from the previous step, it is time to construct the initial structure of PA (including TLs) through the SRFT (Step-3). As the last step in modeling PA, the LSTM-based DNN with the implementation of MOALO algorithm to the output layer is employed as presented in Fig. 2. The input layer consists of specifications of TLs such as: 'W', and 'L'. Hereby, the

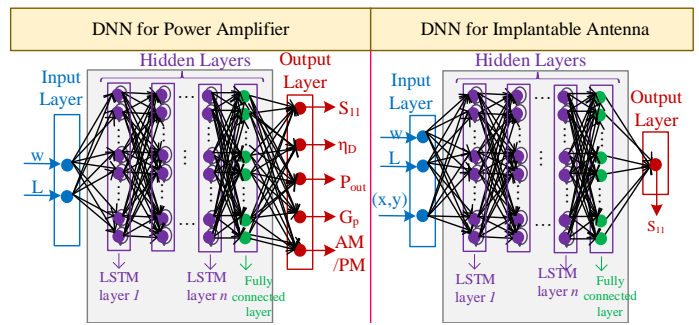


Figure 2: DNN structures for optimizing design parameters of biomedical PA (left-side) and biomedical antenna (right-side).

output layer presents the S_{11} , η_D , P_{out} , G_p and AM/PM specifications for which the MOALO algorithm is employed leading to predict the optimal design parameters of constructed PA (Step-4). More details regarding training and constructing of LSTM-based DNN is presented in Section II.B.a of [28].

After constructing the biomedical PA, it is time to design and optimize the biomedical antenna. The antenna structure incorporates radiators with different lengths, so different resonant frequencies, giving rise to different resonances, hence a wide band antenna. Apart from the coverage of the overall industrial, scientific, and medical (ISM) band, such a wide-band antenna is less sensitive to the variations of the tissue parameters than a narrow-band one. For this case, firstly an automated environment between the EDA tool (here, CST) and numerical analyzer (here, MATLAB) for start designing biomedical antenna is created (Step-5). Afterward, the initial structure of the antenna is generated through a VBA script [29] in which MATLAB prompts the macros in the CST leading to the design antenna automatically (Step-6). After defining the initial configuration of the antenna, the design parameters can be achieved through the trained LSTM-based DNN in which MOALO algorithm is employed (Step-7). As Fig. 2 shows, the constructed related DNN represents specifications as 'W', 'L' (dimensions used in the antenna modeling) and also the position of the feeding point of the antenna as the input layer parameters, whereas the output layer presents the S_{11} specification of the antenna. As the last step, the new GAN network is trained for estimating the RPs of optimized antenna for various frequencies (Step-8).

III. VALIDATION OF THE PROPOSED PARADIGM

The proposed method is validated by arranging the related optimization set-up with the practical CPU execution environment, namely an Intel Core i7-4790 CPU @ 3.60 GHz equipped with 64.0 GB RAM. In this section, firstly the design procedure of a biomedical PA, and secondly the optimized biomedical antenna operating at the center frequency of ISM band, i.e., 2.45 GHz are provided.

A. Biomedical PA design

Figure 3 shows the optimized structure of biomedical PA operating from 2.4 GHz to 2.5 GHz. After constructing the automated environment presented in the previous section, the load-pull extrapolation through the deep image completion

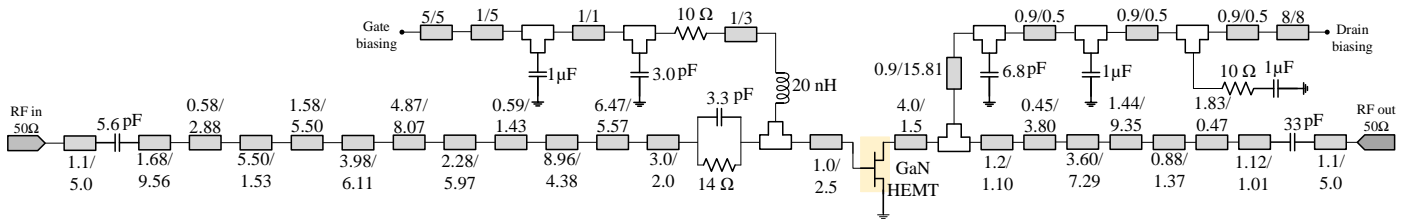


Figure 3: Optimized biomedical PA; all design parameters of TLs (width/length) are in mm unit.

method is employed, since predicting suitable drain and gate impedances is crucial for the SRFT method leading to the construction of the initial structure of PA. Here, full load-pull contours are extrapolated with the help of a partial dataset (i.e., some known impedances) using the GAN network. The depicted GAN network in Fig. 1 is trained by getting the help of extracted 70000 sets of randomly simulated load-pull results with 32×32 -pixel images for which 64 filters are used. For the transposed convolution layers and convolution layers, 5-by-5 filters are determined. The topology of this network is generated by employing Bayesian optimization (BO) [30]. From the predicated impedances, the optimally selected drain and gate impedances to be inserted into the SRFT method are presented in Tab. I. After constructing the structure of the PA, it is time to achieve the optimal design parameters of TLs. For this case, design parameters of PA (i.e., 'W' and 'L' of TLs) are iterated in the range of $\pm 5\%$, $\pm 10\%$, and $\pm 15\%$ results in 5000 data. The hyperparameters of trained LSTM-based DNN are achieved through the BO method. The accuracy of the trained GAN and LSTM-based DNN [31] for the optimized biomedical PA is shown in Fig. 4. The acceptable accuracy for the GAN network is achieved at 1400th epoch and also 0.083 value for the RMSE is obtained at the 200th neuron with 5 hidden layers.

Table I: Predicted load-Pull results at 3-dB gain compression through GAN network; PAE is power added efficiency.

Freq. (GHz)	Gate Impedance	Drain Impedance	PAE (%)	P_{out} (dBm)	G_p (dB)
2.2	0.093-j21.44	23.56 +j24.72	39.97	70.01	14.62
2.3	2.66-j19.51	20.81 +j26.03	39.97	72.32	12.17
2.4	3.92-j16.64	21.02 +j25.93	39.97	74.76	11.77
2.5	5.025-j13.938	19.81 +j24.29	39.97	72.62	11.27
2.6	8.25-j2.38	18.23 +j24.59	39.92	55.29	12.99
2.7	7.94-j2.92	10.67 +j23.30	38.69	48.49	12.39

Figure 5 presents the various outcomes achieved from optimized biomedical PA presented in Fig. 3 in which the design is biased at a drain-source voltage of 50 V with a quiescent drain-source current of 40 mA. The employed substrate is Rogers RO4350B with $\epsilon_r=3.66$ and a thickness of 0.508 mm. The employed transistor is a Wolfspeed CG2H40010F Gallium Nitride (GaN) high-electron mobility transistor (HEMT) results in operating in the frequency band of 2.4 GHz to 2.5 GHz. It is resulting in a G_p higher than 15 dB, and an η_D higher

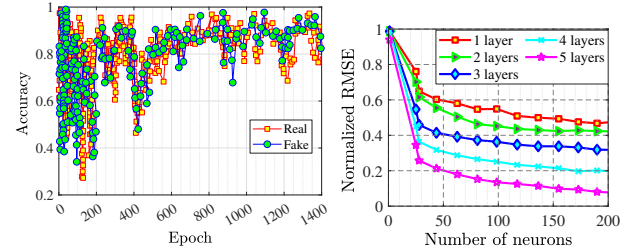


Figure 4: Accuracy representation for GAN with RMSE presentation for optimized PA (right-side).

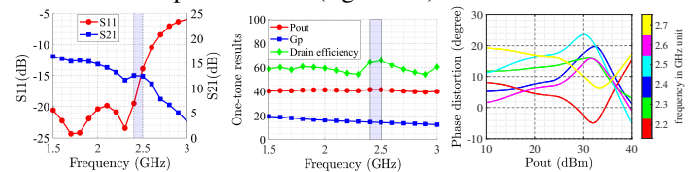


Figure 5: Optimized S-parameter (left-side), one-tone (middle), and phase distortion (right-side) as AM/PM results of biomedical PA operating at center frequency of 2.45 GHz.

than 55% in around 40 dBm P_{out} at 3-dB compression point. Also, it is observed that the phase distortion specification for the optimized PA is performed between 5° and 24° .

B. Biomedical antenna design

Figure 6 represents the optimized configuration of the biomedical antenna that is built on a TiO_2 substrate with the relative permittivity of 95, and for which cover tissue details are specified in Fig. 6 and dispersive electric parameters reported in Fig. 7 (left and middle) [32], [33]. This substrate is selected due to its poorly soluble bio-compatible specification [34]. By getting used to the analysis executed in [35], we utilize average values of the tissue parameters in this work as well. The antenna is designed and optimized on a flat ground plane of dimension of 18 mm \times 16 mm. This configuration is generated automatically by operating CST in the background, handled by MATLAB software, which generates/updates the VBA script describing the antenna geometry. The extension of the superstrate layers are of the same dimension. For a more realistic implementation, a conical configuration as in [33] can also be considered, but is out of the scope of the present investigation.

As Fig. 2 shows, the LSTM-based DNN is constructed for predicting the S_{11} performance of the antenna for the given input specifications. The suitable amount of data for training the network is generated by iterating the design parameters in the range of $[\pm 5\%-\pm 15\%]$ with a step size of $\pm 5\%$. In total 2000 data are generated and hyperparameters of LSTM-based

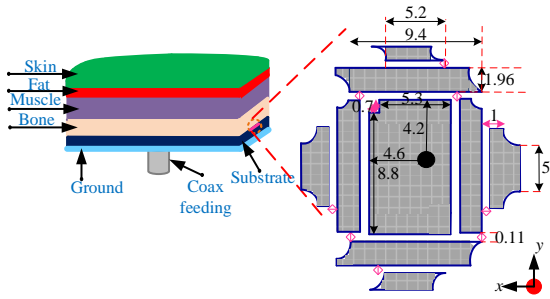


Figure 6: Optimized biomedical antenna.

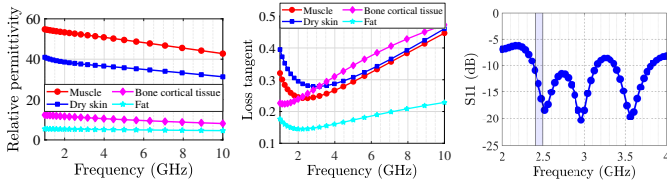


Figure 7: Relative permittivity (left-side), loss tangent for various tissues (middle), and S_{11} performance of optimized biomedical antenna (right-side).

DNN are obtained by the BO method. At this amount of data, acceptable accuracy is achieved. In case of not obtaining the targeted accuracy, the number of data must be increased. This trained LSTM-based DNN predicts the optimal parameters results in the targeted bandwidth of biomedical antenna (see Fig. 7). Afterward, the GAN network is executed for predicting the E-plane and H-plane RPs by extracting 50000 datasets generated randomly by altering the design parameters of the biomedical antenna. The BO method is employed, and hyperparameters like the GAN network for biomedical PA are achieved. The accuracy of LSTM-based DNN is achieved as 0.071 RMSE value at 300th neuron with 3 hidden layers, and the acceptable accuracy for trained GAN is obtained at 1200th epoch as depicted in Fig 8. Respectively, S_{11} with RPs of biomedical antenna are depicted in Fig. 7 and 9 in which the S-parameter outcome is predicated by LSTM-based DNN and RPs are estimated by the trained GAN network. The total consumed time for designing and optimizing biomedical PA with an antenna is around 4 hours and 50 minutes. Figure 10 presents the execution environment for optimizing active and passive devices in which MATLAB is the main core and handling the various impedances extracted from both sides leading to optimizing various output specifications concurrently. Additionally, the effectiveness of our proposed method is proved by making a comparison with genetic algorithm (GA) and particle swarm optimization (PSO) methods with and without neural networks. As potential safety concerns, the proposed method adheres to the safety guidelines in terms of employed transistor model [36], used substrate, and operated bandwidth [33].

IV. CONCLUSION

In this work, we present a fully automated optimization methodology for designing and optimizing active and passive biomedical devices as PA and antenna operating at a center frequency of 2.45 GHz, concurrently. For this case, this method

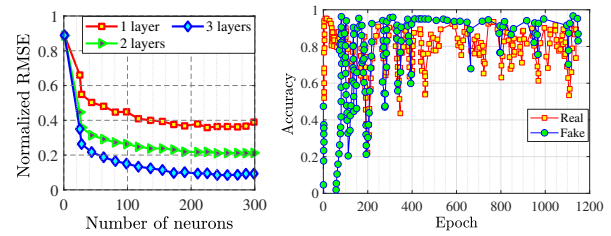


Figure 8: RMSE presentation for optimized biomedical antenna (left-side) with accuracy of trained GAN network (right-side).

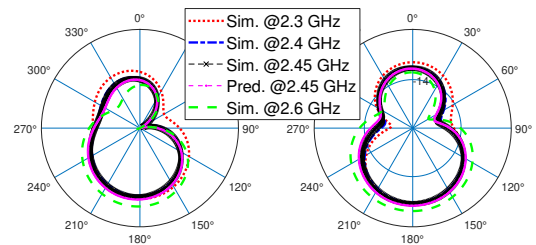


Figure 9: RPs for E-plane (left-side) and H-plane (right-side) at various frequencies; Sim. means simulated and Pred. means predicted.

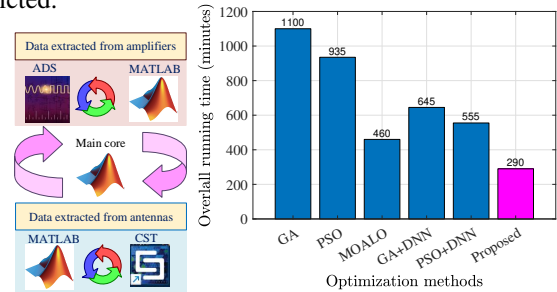


Figure 10: Connection demonstration between EDA tools and numerical analyzers (left-side), comparison between various methods in terms of total consumed time (right-side).

is executed based on the implementation of a deep learning image completion method with the help of GANs and LSTM-based DNNs that are optimized through MOALO algorithm. The constructed GAN network in the biomedical PA side is used for achieving the optimal impedances through load-pull analysis, and the trained GAN network in the biomedical antenna side is employed for extrapolating the RPs. The LSTM-based DNNs are trained for PA and antenna designs to obtain the optimal design parameters. All the processes including constructing the configurations with determining design parameters for both biomedical PA and antenna designs are performed automatically. Some of the challenges that any designer may face are as: i) creating an accurate bridge between various EDA tools, ii) arranging special constraints for used TLs at the PA side for passing EM simulation, iii) selecting appropriate biomedical tissue at antenna side, iv) implementing a successful optimization method in order to fasten the process and not going to the infinite loop. Hence, the proposed strategy will facilitate the time-consuming design and optimization of inside-body WDT transmitters/receivers effectively leading to a reduction the manual breaks. As a future work, implementation of Behavioral models with optimizing the biasing networks of PA are targeted leading to reduced computational time as well.

REFERENCES

- [1] Z. Fang, F. Gao, H. Jin, S. Liu, W. Wang, R. Zhang, Z. Zheng, X. Xiao, K. Tang, L. Lou, K.-T. Tang, J. Chen, and Y. Zheng, "A review of emerging electromagnetic-acoustic sensing techniques for healthcare monitoring," *IEEE Transactions on Biomedical Circuits and Systems*, vol. 16, no. 6, pp. 1075–1094, 2022.
- [2] G.-S. Byun, "A wireless data transfer by using a patch antenna for biomedical applications," *Electronics*, vol. 11, no. 24, 2022. [Online]. Available: <https://www.mdpi.com/2079-9292/11/24/4197>
- [3] S. A. A. Shah, I. A. Shah, S. Hayat, and H. Yoo, "Ultra-miniaturized implantable antenna enabling multiband operation for diverse industrial IoT devices," *IEEE Transactions on Antennas and Propagation*, vol. 72, no. 2, pp. 1352–1362, 2024.
- [4] W. Han, W. Dong, and L. Geng, "A 0.8–5.8 GHz ultra-wideband power amplifier based on dynamic renormalized references," *IEEE Transactions on Circuits and Systems II: Express Briefs*, vol. 71, no. 2, pp. 612–616, 2024.
- [5] A. Egbert, A. Martone, C. Baylis, and R. J. Marks, "Partial load-pull extrapolation using deep image completion," in *2020 IEEE Texas Symposium on Wireless and Microwave Circuits and Systems (WMCS)*, 2020, pp. 1–5.
- [6] J. Jin, Q. Su, Y. Xu, Z. He, and Y. Lu, "Efficient radiation pattern prediction of array antennas based on complex-valued graph neural networks," *IEEE Antennas and Wireless Propagation Letters*, vol. 21, no. 12, pp. 2467–2471, 2022.
- [7] J. Xu, J. S. Filho, S. Nag, L. Long, E. Hwang, C. Tejeiro, G. O'Leary, Y. Huang, M. Kanchwala, M. Abdolrazzagh, C. Tang, P. Liu, Y. Sui, H. You, X. Liu, J. Zariffa, and R. Genov, "Fascicle-selective ultrasound-powered bidirectional wireless peripheral nerve interface IC," *IEEE Transactions on Biomedical Circuits and Systems*, vol. 17, no. 6, pp. 1237–1256, 2023.
- [8] D. N. Elsheikh, O. M. Fahmy, M. Farouk, K. Ezzat, and A. R. Eldamak, "An early breast cancer detection by using wearable flexible sensors and artificial intelligent," *IEEE Access*, vol. 12, pp. 48 511–48 529, 2024.
- [9] A. T. Purnomo, K. S. Komariah, D.-B. Lin, W. F. Hendria, B.-K. Sin, and N. Ahmadi, "Non-contact supervision of covid-19 breathing behaviour with FMCW radar and stacked ensemble learning model in real-time," *IEEE Transactions on Biomedical Circuits and Systems*, vol. 16, no. 4, pp. 664–678, 2022.
- [10] H. Arab, I. Ghaffari, L. Chioukh, S. O. Tatu, and S. Dufour, "A convolutional neural network for human motion recognition and classification using a millimeter-wave doppler radar," *IEEE Sensors Journal*, vol. 22, no. 5, pp. 4494–4502, 2022.
- [11] D. Varam, R. Mitra, M. Mkadmi, R. A. Riyas, D. A. Abuhani, S. Dhou, and A. Alzaatreh, "Wireless capsule endoscopy image classification: An explainable AI approach," *IEEE Access*, vol. 11, pp. 105 262–105 280, 2023.
- [12] X. Jia, X. Xing, Y. Yuan, L. Xing, and M. Q.-H. Meng, "Wireless capsule endoscopy: A new tool for cancer screening in the colon with deep-learning-based polyp recognition," *Proceedings of the IEEE*, vol. 108, no. 1, pp. 178–197, 2020.
- [13] R. Colella, L. Spedicato, L. Laqintana, and L. Catarinucci, "Inertially controlled two-dimensional phased arrays by exploiting artificial neural networks and ultra-low-power ai-based microcontrollers," *IEEE Access*, vol. 11, pp. 23 474–23 484, 2023.
- [14] J. Xiang, M. Xiang, H. Lv, G. Zhou, H. Yang, X. Yu, J. Li, Y. Qin, and S. Fu, "Low-complexity conditional generative adversarial network (C-GAN) based nonlinear equalizer for coherent data-center interconnections," *Journal of Lightwave Technology*, vol. 41, no. 18, pp. 5966–5972, 2023.
- [15] G. L. Barbruni, F. Rodino, P. M. Ros, D. Demarchi, D. Ghezzi, and S. Carrara, "A wearable real-time system for simultaneous wireless power and data transmission to cortical visual prosthesis," *IEEE Transactions on Biomedical Circuits and Systems*, vol. 18, no. 3, pp. 580–591, 2024.
- [16] Y. Zhang, Y. Shao, L. Xiong, and J. Zhang, "An unsupervised learning approach for human activity recognition based on wave propagation in wireless body area networks," in *2023 IEEE International Symposium on Antennas and Propagation and USNC-URSI Radio Science Meeting (USNC-URSI)*, 2023, pp. 1877–1878.
- [17] M. Akrouf, A. Feriani, F. Bellili, A. Mezghani, and E. Hossain, "Domain generalization in machine learning models for wireless communications: Concepts, state-of-the-art, and open issues," *IEEE Communications Surveys Tutorials*, vol. 25, no. 4, pp. 3014–3037, 2023.
- [18] S. Li, F. Xu, and H.-C. Yang, "Reliable and energy-efficient relay transmission in WBANs with wireless power transfer: Optimal design with DRL," in *2024 IEEE Pacific Rim Conference on Communications, Computers and Signal Processing (PACRIM)*, 2024, pp. 1–6.
- [19] V. K. Srivastava, A. Ahmad, and A. Sharma, "A machine learning assisted localization and magnetic field forming for wireless powering of biomedical implant devices," *IEEE Transactions on Antennas and Propagation*, pp. 1–1, 2024.
- [20] S. Yarman, "Design of ultra wideband power transfer networks," *New York, NY, USA: Wiley*, 2010.
- [21] S. Mirjalili, P. Jangir, and S. Saremi, "Multi-objective ant lion optimizer: a multi-objective optimization algorithm for solving engineering problems," *Applied Intelligence*, vol. 46, no. 1, pp. 79–95, Jan 2017. [Online]. Available: <https://doi.org/10.1007/s10489-016-0825-8>
- [22] "Multi-Objective Ant Lion Optimizer (MOALO)," <http://nl.mathworks.com/matlabcentral/fileexchange/58460-multi-objective-ant-lion-optimizer-moalo>, accessed: 2024-05-28.
- [23] K. Kalita, S. B. Pandya, R. Čep, P. Jangir, and L. Abualigah, "Many-objective ant lion optimizer (maoalo): A new many-objective optimizer with its engineering applications," *Heliyon*, vol. 10, no. 12, p. e32911, 2024. [Online]. Available: <https://www.sciencedirect.com/science/article/pii/S2405844024089424>
- [24] I. Goodfellow, J. Pouget-Abadie, M. Mirza, B. Xu, D. Warde-Farley, S. Ozair, A. Courville, and Y. Bengio, "Generative adversarial networks," *Advances in Neural Information Processing Systems*, vol. 3, 06 2014.
- [25] F. Feng, W. Na, J. Jin, J. Zhang, W. Zhang, and Q.-J. Zhang, "Artificial neural networks for microwave computer-aided design: The state of the art," *IEEE Transactions on Microwave Theory and Techniques*, vol. 70, no. 11, pp. 4597–4619, 2022.
- [26] S. Bengesi, H. El-Sayed, M. K. Sarker, Y. Houkpati, J. Irungu, and T. Oladunni, "Advancements in generative AI: A comprehensive review of GANs, GPT, autoencoders, diffusion model, and transformers," *IEEE Access*, vol. 12, pp. 69 812–69 837, 2024.
- [27] H. Ding, N. Huang, Y. Wu, and X. Cui, "Legan: Addressing intraclass imbalance in GAN-based medical image augmentation for improved imbalanced data classification," *IEEE Transactions on Instrumentation and Measurement*, vol. 73, pp. 1–14, 2024.
- [28] L. Kouhalvandi, O. Ceylan, and S. Ozoguz, "Automated deep neural learning-based optimization for high performance high power amplifier designs," *IEEE Transactions on Circuits and Systems I: Regular Papers*, vol. 67, no. 12, pp. 4420–4433, 2020.
- [29] "Automation and scripting | visual basic (vba)," http://https://space.mit.edu/RADIO/CST_online/vba/vba_macro_language_overview.htm, accessed: 2024-05-28.
- [30] S. Greenhill, S. Rana, S. Gupta, P. Vellanki, and S. Venkatesh, "Bayesian optimization for adaptive experimental design: A review," *IEEE Access*, vol. 8, pp. 13 937–13 948, 2020.
- [31] A. K. Rorabaugh, S. Caño-Lores, M. R. W. I. au2, T. Johnston, and M. Tauffer, "Peng4nn: An accurate performance estimation engine for efficient automated neural network architecture search," 2021. [Online]. Available: <https://arxiv.org/abs/2101.04185>
- [32] L. Kouhalvandi, L. Matekovits, and I. Peter, "Multi-band implantable microstrip antenna on large ground plane and TiO2 substrate," in *2021 IEEE 17th International Conference on Wearable and Implantable Body Sensor Networks (BSN)*, 2021, pp. 1–4.
- [33] L. Matekovits, F. Mir, G. Dassano, and I. Peter, "Deeply implanted conformal antenna for real-time bio-telemetry applications," *Sensors*, vol. 24, no. 4, 2024. [Online]. Available: <https://www.mdpi.com/1424-8220/24/4/1170>
- [34] S. Jafari, B. Mahyad, H. Hashemzadeh, S. Janfaza, T. Gholikhani, and L. Tayebi, "Biomedical applications of TiO2 nanostructures: Recent advances," *Int. J. Nanomedicine*, vol. 15, pp. 3447–3470, May 2020.
- [35] G. Strnad, L. Jakob-Farkas, F. S. Gobber, and I. Peter, "Synthesis and characterization of nanostructured oxide layers on Ti-Nb-Zr-Ta and Ti-Nb-Zr-Fe biomedical alloys," *Journal of Functional Biomaterials*, vol. 14, no. 4, 2023. [Online]. Available: <https://www.mdpi.com/2079-4983/14/4/180>
- [36] C. Li, X. Chen, and Z. Wang, "Review of the AlGaIn/GaN high-electron-mobility transistor-based biosensors: Structure, mechanisms, and applications," *Micromachines*, vol. 15, no. 3, 2024. [Online]. Available: <https://www.mdpi.com/2072-666X/15/3/330>